IRES–GFP and MSCV-dH-IRES–GFP). The dS, dA and dH mutants lack the S region (amino acid residues 267–322), the A region (residues 313–382) and H region (residues 383–525), respectively. We created MSCV-IL-7Rα-IRES–GFP by inserting a mouse IL-7Rα cDNA into the *Xho*I site of MSCV-IRES–GFP. To generate the MSCV-GMRα-IRES-β_c vector, we inserted human GMRα cDNA into the *Xho*I site of the MSCV-IRES–GFP vector (MSCV-GMRα-IRES–GFP) and put the human β_c cDNA downstream of the IRES in place of the GFP cDNA. A retroviral vector for EpoR (MSCV-EpoR-IRES–GFP)[28] was provided by G. Q. Daley.

Retroviral gene transfer

We produced virus from a packaging cell line, Phoenix, by transient transfection of MSCV constructs with FuGENE 6 (Roche Molecular Biochemicals). For viral infection, CLPs were cultured at 5,000 cells per well in a 96-well round-bottomed plate with 50% virus stock in Iscove's Modified Dulbecco's Media (IMDM) containing 10% FCS, 50 μM 2-mercaptoethanol, 4 μg ml^{-1} polybrene, SlF (20 ng ml^{-1}), FL (20 ng ml^{-1}) and IL-7 (10 ng ml^{-1}) for 12 h at 32 °C. Cells were further cultured for 36–48 h at 37 °C to allow exogenous gene expression. Human IL-2 (25 ng ml^{-1}), erythropoietin (4 U ml^{-1}) and GM-CSF (20 ng ml^{-1}) were used in this culture for stimulating the human IL-2Rβ-, EpoR- and GM-CSFR-expressing CLPs, respectively.

In vitro cell culture

Between 1 and 40 CLPs were sorted by the automatic cell deposition unit (ACDU, Beckton Dickinson) on the FACS Vantage. The cells were cultured in 96-well plates on an OP9 stromal layer in the presence of indicated cytokines for 7–10 days. Methylcellulose culture was done as described[5].

RT–PCR analysis

We isolated RNA from cells with Trizol reagent (GIBCO BRL). Oligo-dT primed cDNA was subjected to PCR. After electrophoresis with 2% agarose gel, bands were detected by ethidium bromide staining. Amplified bands for human GM-CSFRα were detected by Southern blotting with the radiolabelled synthesized oligo as a probe. For the primer sequence, see Supplementary Information.

Receive 22 May; accepted 31 July 2000.

1. Fairbairn, L. J., Cowling, G. J., Reipert, B. M. & Dexter, T. M. Suppression of apoptosis allows differentiation and development of a multipotent hemopoietic cell line in the absence of added growth factors. *Cell* **74,** 823–832 (1993).
2. Ogawa, M. Differentiation and proliferation of hematopoietic stem cells. *Blood* **81,** 2844–2853 (1993).
3. Watowich, S. S. *et al.* Cytokine receptor signal transduction and the control of hematopoietic cell development. *Annu. Rev. Cell Dev. Biol.* **12,** 91–128 (1996).
4. Metcalf, D. Stem cells, pre-progenitor cells and lineage-committed cells: are our dogmas correct? *Ann. NY Acad. Sci.* **872,** 289–303 (1999); discussion **872,** 303–304 (1999).
5. Kondo, M., Weissman, I. L. & Akashi, K. Identification of clonogenic common lymphoid progenitors in mouse bone marrow. *Cell* **91,** 661–672 (1997).
6. Ogasawara, K. *et al.* Requirement for IRF-1 in the microenvironment supporting development of natural killer cells. *Nature* **391,** 700–703 (1998); erratum **392,** 843 (1998).
7. Lodolce, J. P. *et al.* IL-15 receptor maintains lymphoid homeostasis by supporting lymphocyte homing and proliferation. *Immunity* **9,** 669–676 (1998).
8. Kennedy, M. K. *et al.* Reversible defects in natural killer and memory CD8 T cell lineages in interleukin 15-deficient mice. *J. Exp. Med.* **191,** 771–780 (2000).
9. Giri, J. G. *et al.* Utilization of the beta and gamma chains of the IL-2 receptor by the novel cytokine IL-15. *EMBO J.* **13,** 2822–2830 (1994).
10. Sugamura, K. *et al.* The interleukin-2 receptor gamma chain: its role in the multiple cytokine receptor complexes and T cell development in XSCID. *Annu. Rev. Immunol.* **14,** 179–205 (1996).
11. Kondo, M. *et al.* Sharing of the interleukin-2 (IL-2) receptor gamma chain between receptors for IL-2 and IL-4. *Science* **262,** 1874–1877 (1993).
12. Nemoto, T. *et al.* Differences in the interleukin-2 (IL-2) receptor system in human and mouse: alpha chain is required for formation of the functional mouse IL-2 receptor. *Eur. J. Immunol.* **25,** 3001–3005 (1995).
13. Asano, M. *et al.* IL-2 can support growth of CD8+ T cells but not CD4+ T cells of human IL-2 receptor beta-chain transgenic mice. *J. Immunol.* **153,** 5373–5381 (1994).
14. Nakano, T., Kodama, H. & Honjo, T. Generation of lymphohematopoietic cells from embryonic stem cells in culture. *Science* **265,** 1098–1101 (1994).
15. Domen, J., Gandy, K. L. & Weissman, I. L. Systemic overexpression of BCL-2 in the hematopoietic system protects transgenic mice from the consequences of lethal irradiation. *Blood* **91,** 2272–2282 (1998).
16. Henry, C., Marbrook, J., Vann, D. C., Kodlin, D. & Wofsy, C. in *Selected Methods in Cellular Immunology* (eds Mishell, B. B. & Shiigi, S. M.) 138–152 (WH Freeman, San Francisco, 1981).
17. Schlissel, M. S. & Stanhope-Baker, P. Accessibility and the developmental regulation of V(D)J recombination. *Semin. Immunol.* **9,** 161–170 (1997).
18. Hatakeyama, M., Mori, H., Doi, T. & Taniguchi, T. A restricted cytoplasmic region of IL-2 receptor beta chain is essential for growth signal transduction but not for ligand binding and internalization. *Cell* **59,** 837–845 (1989).
19. Nelson, B. H. & Willerford, D. M. Biology of the interleukin-2 receptor. *Adv. Immunol.* **70,** 1–81 (1998).
20. Constantinescu, S. N., Ghaffari, S. & Lodish, H. F. The erythropoietin receptor: structure, activation and intracellular signal transduction. *Trends Endocrinol. Metab.* **10,** 18–23 (1999).
21. Watanabe, S. *et al.* Reconstituted human granulocyte-macrophage colony-stimulating factor receptor transduces growth-promoting signals in mouse NIH 3T3 cells: comparison with signalling in BA/F3 pro-B cells. *Mol. Cell. Biol.* **13,** 1440–1448 (1993).
22. Ha, K., Minden, M., Hozumi, N. & Gelfand, E. W. Immunoglobulin gene rearrangement in acute myelogenous leukemia. *Cancer Res.* **44,** 4658–4660 (1984).
23. Palumbo, A., Minowada, J., Erikson, J., Croce, C. M. & Rovera, G. Lineage infidelity of a human myelogenous leukemia cell line. *Blood* **64,** 1059–1063 (1984).
24. Cheng, G. Y., Minden, M. D., Toyonaga, B., Mak, T. W. & McCulloch, E. A. T cell receptor and immunoglobulin gene rearrangements in acute myeloblastic leukemia. *J. Exp. Med.* **163,** 414–424 (1986).
25. Godfrey, D. I., Kennedy, J., Mombaerts, P., Tonegawa, S. & Zlotnik, A. Onset of TCR-beta gene rearrangement and role of TCR-beta expression during CD3$^-$CD4$^-$CD8$^-$ thymocyte differentiation. *J. Immunol.* **152,** 4783–4792 (1994).
26. Hardy, R. R., Carmack, C. E., Shinton, S. A., Kemp, J. D. & Hayakawa, K. Resolution and characterization of pro-B and pre-pro-B cell stages in normal mouse bone marrow. *J. Exp. Med.* **173,** 1213–1225 (1991).
27. Rolink, A. *et al.* A subpopulation of B220+ cells in murine bone marrow does not express CD19 and contains natural killer cell progenitors. *J. Exp. Med.* **183,** 187–194 (1996).
28. Ghaffari, S. *et al.* BCR-ABL and v-SRC tyrosine kinase oncoproteins support normal erythroid development in erythropoietin receptor-deficient progenitor cells. *Proc. Natl Acad. Sci. USA* **96,** 13186–13190 (1999).

Supplementary information is available on *Nature*'s World-Wide Web site (http://www.nature.com) or as paper copy from the London editorial office of *Nature*.

Acknowledgements

We thank T. Honjo for IL-2Rβ transgenic mice; G. Nolan for the retroviral system; S. Watanabe for cDNAs for human GM-CSFRα and β_c; G. Q. Daley for a retroviral expression vector for EpoR; S.-I. Nishikawa for OP9 cells and anti-IL-7Rα antibody; and L. Jerabek for laboratory management. This work was supported by USPHS grant to I.L.W, and a Jose Carreras International Leukemia Foundation Grant to K.A. M.K., D.C.S. and A.G.K. are supported by fellowships from the Irvington Institute for Immunology, American Cancer Society California Division, and USPHS Training Grant, respectively.

Correspondence and requests for materials should be addressed to M.K. (e-mail: motonari.kondo@stanford.edu).

Tat-specific cytotoxic T lymphocytes select for SIV escape variants during resolution of primary viraemia

Todd M. Allen*†, David H. O'Connor*†, Peicheng Jing*, John L. Dzuris‡, Bianca R. Mothé*, Thorsten U. Vogel*, Ed Dunphy*, Max E. Liebl*, Carol Emerson*, Nancy Wilson*, Kevin J. Kunstman‖, Xiaochi Wang¶, David B. Allison#, Austin L. Hughes☆, Ronald C. Desrosiers, John D. Altman¶, Steven M. Wolinsky‖, Alessandro Sette‡ & David I. Watkins*††**

** Wisconsin Regional Primate Research Center, University of Wisconsin, 1220 Capitol Court, Madison, Wisconsin 53715-1299, USA*
‡ Epimmune, 5820 Nancy Ridge Drive, San Diego, California 92121, USA
‖ Northwestern University Medical School, 303 East Chicago, Room 3-735 Tarry Building, Chicago, Illinois 60611-3008, USA
¶ Emory Vaccine Center, Emory University School of Medicine, G211 Rollins Research Building, 1510 Clifton Road, Atlanta, Georgia 30322, USA
 # St. Luke's/Roosevelt Hospital, Obesity Research Center, 1090 Amsterdam Avenue, Suite 14B, New York, New York 10025, USA
☆ Department of Biological Sciences, 401 Coker Life Sciences, University of South Carolina, Columbia, South Carolina 29208, USA
*** New England Regional Primate Research Center, One Pine Hill Drive, Southborough, Massachusetts 01772-9102, USA*
†† Dept. of Pathology and Laboratory Medicine, University of Wisconsin, 1300 University Avenue, Madison, Wisconsin 53706-1532, USA
† These authors contributed equally to this work

Human immunodeficiency virus (HIV) and simian immunodeficiency virus (SIV) infections are characterized by early peaks of viraemia that decline as strong cellular immune responses develop[1,2]. Although it has been shown that virus-specific CD8-positive cytotoxic T lymphocytes (CTLs) exert selective pressure during HIV and SIV infection[3–11], the data have been controversial[12,13]. Here we show that Tat-specific CD8-positive T-lymphocyte responses select for new viral escape variants during

the acute phase of infection. We sequenced the entire virus immediately after the acute phase, and found that amino-acid replacements accumulated primarily in Tat CTL epitopes. This implies that Tat-specific CTLs may be significantly involved in controlling wild-type virus replication, and suggests that responses against viral proteins that are expressed early during the viral life cycle might be attractive targets for HIV vaccine development.

The strongest CD8-positive T lymphocyte responses to HIV and SIV are observed in the first few weeks of infection, coincident with the initial decline in plasma viraemia. We reasoned that viral escape might occur from immune responses that exert selective pressure during this acute phase of infection. To test this hypothesis, we examined viral evolution during acute infection of 18 rhesus macaques with molecularly cloned SIV.

Every animal (10/10) expressing the rhesus major histocompatibility (MHC) class I molecule Mamu-A*01 made CD8-positive T-lymphocyte responses, which peaked between 3 and 4 weeks after infection, to a newly defined epitope in $Tat_{28–35}$ STPESANL[14] (SL8, Fig. 1). In two of these animals, up to 10% of their CD8/CD3-positive lymphocytes recognized this Tat epitope. However, the frequency of Tat-specific lymphocytes declined precipitously after the acute phase (Fig. 1). We reasoned that this decline might be the result of viral escape from these Tat-specific responses. We investigated this possibility by sequencing the 5′ exon of Tat using virus derived from the ten Mamu-A*01-positive animals. By 8 weeks after infection, a high frequency of amino-acid substitution was observed in the SL8 epitope (Fig. 2a). Eighty-six per cent of clones contained variation in the CD8-positive T-lymphocyte epitope at this time point. In five out of the ten Mamu-A*01-positive animals, all sequenced clones contained mutations in the Mamu-A*01-restricted SL8 epitope. In contrast, little amino-acid variation was observed outside this SL8 epitope in Mamu-A*01-positive animals (Fig. 2b).

We then investigated whether these changes in the SL8 epitope resulted from a mixed population of variants in our inocula or whether they were selected for increased replicative fitness in Mamu-A*01-negative animals. As expected from a molecular clone, there was little variation in this epitope in either of the two inocula (Fig. 2a). In addition, only one out of eight Mamu-A*01-negative animals exhibited changes in the SL8 epitope (see Supplementary Information, Fig. 1). Thus, viral escape from the Mamu-A*01-restricted Tat-specific CD8-positive T-lymphocyte responses appeared to be the most consistent explanation for our findings.

We then performed a time-course analysis of viral evolution within the SL8 epitope and sequenced the entire virus after the acute phase in two of the Mamu-A*01-positive animals. At peak viraemia (2 weeks after infection), Tat-specific CTL responses were barely detectable and no changes in the Mamu-A*01-bound Tat epitope were present (Fig. 2c, d). After resolution of peak viraemia (3 weeks after infection), Tat-specific CD8-positive T lymphocytes were at their highest level. One week later, extensive variation was apparent in the virus populations of both animals (Fig. 2c, d). Furthermore, direct sequencing of the open reading frames of the entire virus at 4 weeks after infection revealed only a single site of viral nucleotide diversity in the SL8 epitope in animal 96118. In animal 96114 there were three sites of viral nucleotide diversity, one of which was in the SL8 epitope, and the other two in Rev and Env (see Supplementary Information; Fig. 2). In animal 96118, the nucleotide substitution in RNA encoding the SL8 epitope caused a change in the overlapping reading frame of Vpr. In animal 96114, the change in Rev also caused a substitution in the overlapping open reading frame of Env. This Rev replacement is seen in most animals infected with this viral clone and appears to be selected for increased viral fitness. Analysis of the additional replacement in animal 96114 in Env by interferon-γ enzyme-linked immunospot (ELISPOT) assays of CD8 and CD4 lymphocytes, however, failed to show conclusively that this region contained any T-cell epitopes.

To determine whether the observed sequence changes in the SL8 epitope do represent viral escape variants, we characterized the functional consequences of the predominant variant epitopes on peptide binding to Mamu-A*01 and on CTL recognition. *In vitro* peptide-binding analyses showed that the new variants of the SL8 epitope did not bind as well as the wild-type peptide to Mamu-A*01 (Table 1). The substitutions of proline at P1 and leucine at P5 reduced peptide binding by more than 50% and 80%, respectively. The isoleucine substitution at P2 and the glutamine, arginine and proline substitutions at P8 abrogated binding (> 99% reduction). As P2 is a secondary anchor and P8 is the carboxy anchor[15] for peptides bound by the Mamu-A*01 molecule, we would expect

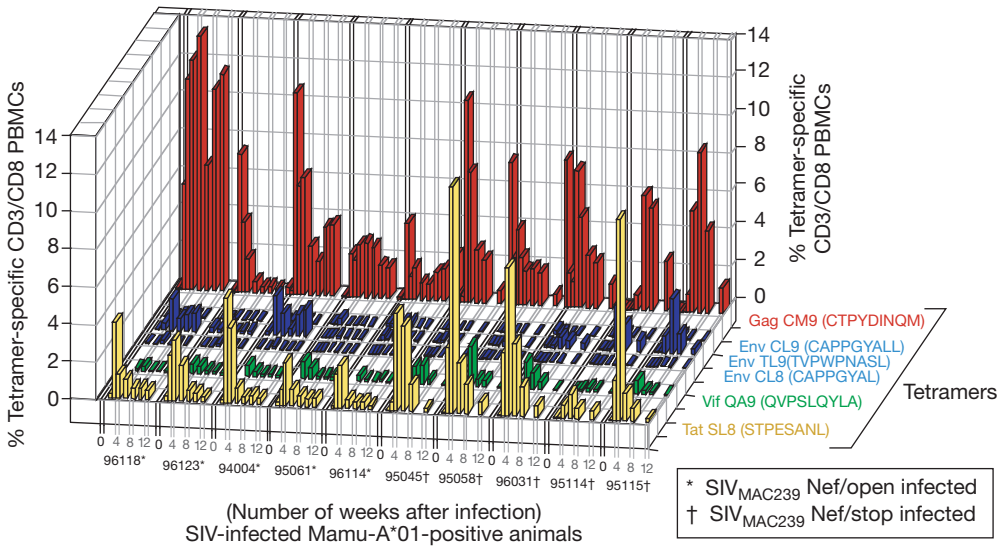

Figure 1 Quantitation of CD8-positive T-lymphocyte responses to various Mamu-A*01-bound peptides. The comparison of CD8-positive T-lymphocyte responses to 6 different epitopes in 10 Mamu-A*01-positive SIV-infected macaques during the first 12 weeks of infection shows that there is a strong CD8-positive T-lymphocyte response to Tat during the acute phase. The Mamu-A*01 Tat_{28-35} tetramer was initially constructed using an SIV_{MAC251}-derived peptide (TTPESANL). This tetramer detected strong responses during the acute phase of SIV_{MAC239}-infected macaques, even though the corresponding SIV_{MAC239} sequence was STPESANL. Subsequent staining with the $Tat_{28–35}$ STPESANL tetramer yielded identical results (data not shown).

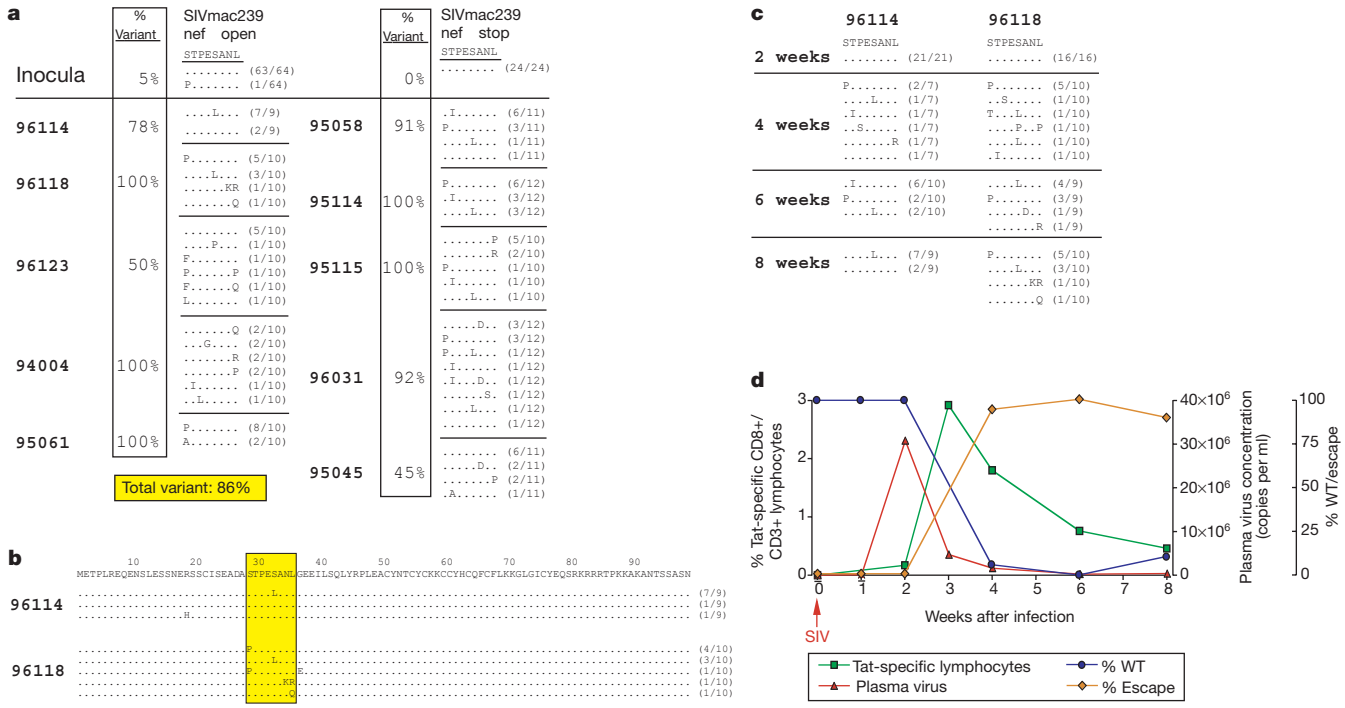

Figure 2 Variation is present in the SL8 epitope of all 10 Mamu-A*01-positive animals after acute SIV infection using analysis of clones isolated from plasma virus. **a**, Variation in the SL8 epitope in Mamu-A*01-positive animals infected with molecularly cloned SIV_{MAC239} Nef stop or SIV_{MAC239} Nef open. Limited variation is detectable in the inocula. The predicted amino-acid translation of a minimum of 9 clones isolated 6–8 weeks after infection is shown. The frequency of the epitope variant is shown to the right of the sequence. **b**, Little variation outside the SL8 epitope in the 5′ exon of Tat in Mamu-A*01-positive animals. The entire 5′ exon of Tat in two Mamu-A*01-positive animals is shown. Amino-acid substitutions accumulate primarily in the STPESANL epitope during the first 8 weeks of infection. **c**, Viral populations in the Mamu-A*01-restricted SL8 epitope evolve rapidly during the acute phase. Predicted amino-acid sequences of virus derived 2, 4, 6 and 8 weeks after infection in animals 96114 and 96118. By 4 weeks after infection, sequence variation was detectable within the epitope. **d**, Temporal relationships between viral load, tetramer levels and the percentage of wild-type and escaped virus. Values were averaged for animals 96114 and 96118, illustrating that loss of wild-type virus is coincident with the peak of tetramer levels and with the decline in plasma virus concentrations.

substitutions at anchor residues to have the most profound effect on peptide binding. Similarly, analyses of CTL lines generated from the peripheral blood mononuclear cells (PBMCs) of several Mamu-A*01-positive animals stimulated with the SL8 index peptide poorly recognized the new variant epitopes (Fig. 3). Notably, variant peptides with the P5 leucine substitution were the least efficient at sensitizing targets for CTL lysis, suggesting that this P5 mutation was probably interfering with T-cell receptor (TCR) recognition. Therefore, it seems probable that the new variants either reduced the amount of Tat-derived peptide/MHC class I complexes on the cell surface or reduced the ability of these complexes to be recognized by the T-cell receptor[16].

To test the hypothesis that viruses with amino-acid replacements within the SL8 epitope are favoured by natural selection, we compared the number of synonymous nucleotide substitutions per synonymous site (d_S) and the number of non-synonymous nucleotide substitutions per non-synonymous site (d_N) in the epitope and in the remainder of the sequence. In the SL8 epitope region of the virus from Mamu-A*01-positive animals, mean d_N was significantly higher than mean d_S both for comparisons between samples and the inoculum ($d_N = 5.7 \pm 0.4$; $d_S = 0.4 \pm 0.4$, $P < 0.001$) and in comparisons within samples ($d_N = 7.3 \pm 1.0$; $d_S = 0.7 \pm 0.7$, $P < 0.001$; see Supplementary Information, Table 1). Mean d_N values in the SL8 epitope from Mamu-A*01-positive animals were almost 60-fold greater than the corresponding values for Mamu-A*01-negative animals ($d_N = 5.7$ in Mamu-A*01-positive animals; $d_N = 0.1$ in Mamu-A*01-negative animals). As a pattern of $d_N > d_S$ is not expected under neutral evolution[4,17,18], this result strongly implies that amino-acid replacements in the SL8 epitope are favoured by positive darwinian selection.

Notably, the 5′ exon of four of the eight Mamu-A*01-negative animals showed patterns of variation suggestive of escape from other Tat-specific cellular immune responses (see Supplementary Information, Figs 1 and 3). We therefore explored the possibility

Table 1 Peptide binding of mutant Tat epitopes to the rhesus MHC class I molecule Mamu-A*01

		IC_{50}*	Relative binding† (mean)	(s.d.)	% Binding reduction‡
Tat_{28-35} epitope (index)	STPESANL	43	1	0	0
Variant	P.......	100	0.43	0.025	67
Variant	.I.....	4,611	0.009	0.001	>99
Variant	....L...	281	0.155	0.03	85
Variant	.......Q	13,175	0.003	0.0004	>99
Variant	.......P	4,573	0.009	0.004	>99
Variant	.......R	15,091	0.003	0.0012	>99

* ^{125}I-labelled peptide: ATPYDINQML.
† Relative peptide binding is expressed relative to the binding affinity of the Tat_{28-35} STPESANL to the rhesus macaque MHC class I molecule Mamu-A*01.
‡ The percentage binding reduction is calculated as (1.0 – relative binding average) × 100.

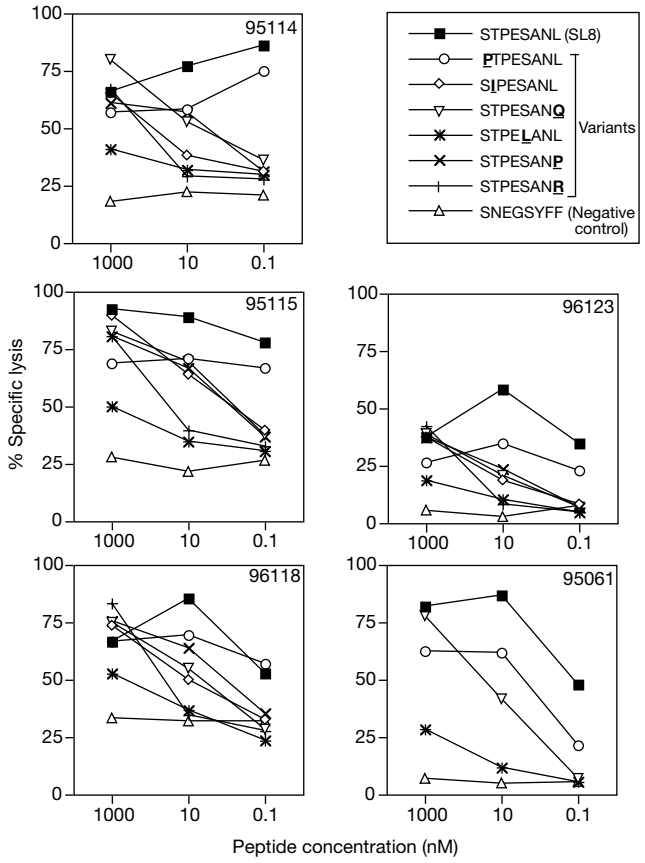

Figure 3 CTL analyses of CD8-positive T-lymphocytes stimulated with the SL8 peptide. Cell lines were stimulated with the index peptide (SL8) and autologous B-LCL. After 2 weeks in culture, these T-cell lines were used in CTL analyses at an effector:target (E:T) ratio of 25:1 with the index peptide and the variants. Three different dilutions of peptides were tested.

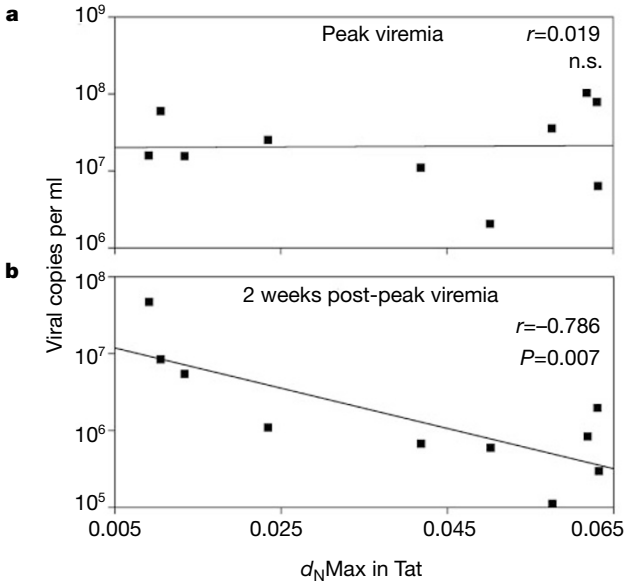

Figure 4 Inverse correlation between plasma viral concentrations and peak d_N in Tat. Peak d_N in Tat was plotted against plasma viral concentrations at peak viraemia and at 2 weeks after peak viraemia, revealing a significant inverse correlation between peak d_N and viral concentration at 2 weeks after peak viraemia.

that animals with little evidence for selection in Tat should have higher plasma virus concentrations than animals with evidence for increased d_N in Tat. As the 18 animals in our cohort were originally part of a vaccine study[19], we excluded the 8 Mamu-A*01-positive animals that had been vaccinated from this analysis. The two naive Mamu-A*01-positive and four of the naive Mamu-A*01-negative animals exhibited evidence of increased d_N peaks within the 5′ exon of Tat, whereas four Mamu-A*01-negative naive animals revealed little evidence of increased d_N in Tat (see Supplementary Information, Fig. 4). Averaging the plasma virus concentrations of these two groups of animals showed a significant difference of at least one log ($P = 0.008$) between the plasma virus concentrations of animals with high and low d_N in Tat at 2 and 4 weeks after peak viraemia (see Supplementary Information, Fig. 5). Similarly, a significant inverse correlation was observed between peak d_N and viral load 2 weeks ($P = 0.007$), 4 weeks ($P = 0.008$) and 8 weeks ($P = 0.048$) after peak viraemia (Fig. 4; and data not shown). Of the four animals with low d_N in Tat, two rapidly progressed to simian AIDS and had SIV plasma virus concentrations in excess of 100×10^6 copies per ml within 6 months of infection. Therefore, animals with evidence of increased d_N in Tat may have controlled wild-type virus better than those with less selective pressure on Tat.

Vaccine-induced cellular immune responses against proteins expressed early in the viral life cycle may be better able to control HIV and SIV replication than responses directed against proteins that are expressed later in the viral life cycle. Viral escape from Tat-specific CD8-positive T lymphocytes occurred with kinetics similar to those seen during the emergence of drug-resistant mutants[20]. In five out of ten Mamu-A*01-positive animals, all clones isolated from plasma at 6–8 weeks after infection contained mutations in the Mamu-A*01-restricted SL8 epitope. This implies that Tat-specific CD8-positive T lymphocytes efficiently controlled replication of the original wild-type inoculum virus in these five animals. Responses directed against early proteins such as Tat may be particularly effective at controlling initial virus replication, as Tat and Rev are the only two viral proteins produced before Nef downregulates MHC class I molecules[21]. Tat-specific CTLs may, therefore, be potent inhibitors of early viral replication, whereas CTLs directed against peptides derived from other viral proteins may find few MHC class I/peptide complexes on the cell surface later in the course of the viral life cycle. The differences between the Gag and Tat-specific CTLs in their ability to exert selective pressure favouring viral escape are intriguing. Understanding the qualitative differences between these CTLs that account for these characteristics will be an important issue in the design of an effective HIV vaccine. Interestingly, vaccination of non-human primates with either Tat protein[22,23] or recombinant viruses expressing Tat and Rev[24] have reduced virus replication. In these studies it is possible that Tat-specific CD8-positive T-lymphocyte responses were involved in control of viral replication. □

Methods

Tetramer analysis

Soluble tetrameric Mamu-A*01 MHC class I/SIV peptide complexes were constructed as described[14,25]. Background tetramer staining of fresh, unstimulated PBMCs from naive Mamu-A*01-positive animals was routinely less than 0.08%.

Amplification of viral RNA from plasma and sequence detection

We obtained SIV plasma virus sequence as described[7]. The primers used to amplify complementary DNA encoding the Mamu-A*01 Tat epitope included SIV 6511-F (5′-TGATCCTCGCTTGCTAACTG-3′) and 6900-R (5′-AGCAAGATGGCGATAAGCAG-3′). These primers were then used to isolate and sequence the cloned inserts. Seven overlapping PCR primer pairs (see Supplementary Information, Fig. 2b) were used to amplify cDNA spanning the entire SIV genome. The PCR products were directly sequenced from both cDNA strands. Overlapping sequence between the primers linked together sequences from the individual RT–PCR reactions. Sequence editing and finishing was performed using Auto Assembler v2.1 on a Macintosh. Nucleotide and predicted amino-acid sequences were aligned using MacVector 4.1 (Oxford Molecular).

Mamu-A*01 binding assay

We carried out quantitative assays for the binding of peptides to soluble Mamu-A*01 molecules on the basis of the inhibition of binding of a radiolabelled standard probe peptide to detergent-solubilized MHC molecules[15]. We used a position-1 C→A mutant of the SIV Gag 181–190 peptide (ATPYDINQML) as the radiolabelled probe. In the case of competitive assays, the concentration of peptide yielding 50% inhibition of the binding of the radiolabelled probe peptide was calculated. We initially tested peptides at one or two high doses. The half-maximal inhibitory concentration (IC_{50}) of peptides yielding positive inhibition were then determined in subsequent experiments, in which 2–6 further dilutions were tested, as necessary. Because, under the conditions we used, where [label] $<$ [MHC] and $IC_{50} \approx$ [MHC], the measured IC_{50} values are reasonable approximations of the true K_d values. Each competitor peptide was tested in 2–4 completely independent experiments. As a positive control, in each experiment we tested the unlabelled version of the radiolabelled probe and measured its IC_{50}.

Generation of *in vitro* cultured CTL effector cells

We established CTL cultures from peripheral blood samples of SIV-infected rhesus macaques drawn in EDTA tubes, and cultured and assayed CTLs as described[7].

Animals, viruses and infections

Rhesus macaques used in this study were identified as *Mamu-A*01*$^+$ by PCR with sequence-specific primers (SSP) and direct sequencing as described[26]. All rhesus macaques used in this study were Mamu-A*01-positive, with the exception of animals 95003, 95112, 96020, 96081, 96093, 96072, 96104 and 96113. Rhesus macaques 95045, 96031, 95058, 96118, 96123, 95061, 96114 and 94004 were vaccinated with a DNA/Modified Vaccinia Ankara (MVA) regimen expressing the $Gag_{181–189}$ peptide (CTPYDINQM)[19]. The Mamu-A*01-positive macaques 95114 and 95115 were not vaccinated before challenge. All rhesus macaques were infected intrarectally with a molecularly cloned virus; SIV_{MAC239} (ref. 27) either Nef stop (95045, 96031, 95058, 95114, 95115, 95003 and 95112) or Nef open (99118, 96123, 95061, 96114, 94004, 96020, 96081, 96093, 96072, 96104 and 96113)). Plasma viral concentrations were measured by branched DNA analysis (Chiron). The virus stock was amplified on rhesus PBMCs only. SIV-infected animals were cared for according to an experimental protocol approved by the University of Wisconsin Research Animal Resource Committee.

Statistical analysis of sequence and plasma virus concentration data

Numbers of synonymous nucleotide substitutions per synonymous site (d_S) and of non-synonymous nucleotide substitutions per non-synonymous site (d_N) were estimated as described[28]. For the sample of viral sequences taken from a given animal, the means of d_S and d_N were computed for (1) all pairwise comparisons between each viral sequence and viral sequences sampled from the inoculum; and (2) all pairwise comparisons among viral sequences within the sample. These quantities were computed for the $Tat_{28–35}$ epitope and the remainder of the 98-codon portion of Tat that was sequenced. To evaluate the statistical significance of the difference in peak and post-peak viraemia between macaques with high and low d_N in Tat, we compared the natural log (that is, ln) plasma virus concentrations among animals with high and low d_N. Taking ln greatly improved the fit of the data to the assumptions of the statistical models used (that is, normality, homoscedasticity in a multivariate test). We also used multiple analysis of variance (MANOVA) which is dependent on fewer assumptions than the repeated measures ANOVA.

Received 10 May; accepted 11 July 2000.

1. Koup, R. A. *et al.* Temporal association of cellular immune responses with the initial control of viremia in primary human immunodeficiency virus type 1 syndrome. *J. Virol.* **68,** 4650–4655 (1994).
2. Yasutomi, Y., Reimann, K., Lord, C., Miller, M. & Letvin, N. Simian immunodeficiency virus-specific CD8+ lymphocyte response in acutely infected rhesus monkeys. *J. Virol.* **67,** 1707–1711 (1993).
3. Goulder, P. J. R. *et al.* Late escape from an immunodominant cytotoxic T-lymphocyte response associated with progression to AIDS. *Nature Med.* **3,** 212–217 (1997).
4. Wolinsky, S. M. *et al.* Adaptive evolution of human immunodeficiency virus-type 1 during the natural course of infection. *Science* **272,** 537–542 (1996).
5. Koenig, S. *et al.* Transfer of HIV-1-specific cytotoxic T lymphocytes to an AIDS patient leads to selection for mutant HIV variants and subsequent disease progression. *Nature Med.* **1,** 330–336 (1995).
6. Mortara, L. *et al.* Selection of virus variants and emergence of virus escape mutants after immunization with an epitope vaccine. *J. Virol.* **72,** 1403–1410 (1998).
7. Evans, D. T. *et al.* Virus-specific CTL responses select for amino acid variation in SIV Env and Nef. *Nature Med.* **5,** 1270–1276 (1999).
8. Phillips, R. E. *et al.* Human immunodeficiency virus genetic variation that can escape cytotoxic T cell recognition. *Nature* **354,** 453–459 (1991).
9. Couillin, I. *et al.* Impaired cytotoxic T lymphocyte recognition due to genetic variations in the main immunogenic region of the human immunodeficiency virus 1 NEF protein. *J. Exp. Med.* **180,** 1129–1134 (1994).
10. Price, D. A. *et al.* Positive selection of HIV-1 cytotoxic T lymphocyte escape variants during primary infection. *Proc. Natl Acad. Sci. USA* **94,** 1890–1895 (1997).
11. Borrow, P. *et al.* Antiviral pressure exerted by HIV-1-specific cytotoxic T lymphocytes (CTLs) during primary infection demonstrated by rapid selection of CTL escape virus. *Nature Med.* **3,** 205–211 (1997).
12. Balter, M. Modest Briton stirs up storm with views on role of CTLs. *Science* **280,** 1860–1861 (1998).
13. Meyerhans, A. *et al. In vivo* persistence of a HIV-1-encoded HLA-B27-restricted cytotoxic T lymphocyte epitope despite specific *in vitro* reactivity. *Eur. J. Immunol.* **21,** 2637–2640 (1991).
14. Allen, T. M. *et al.* CD8+ lymphocytes from SIV-infected rhesus macaques recognize 27 different peptides bound by a single MHC class I molecule: Implications for vaccine design and testing. *J. Virol.* (in the press).
15. Allen, T. M. *et al.* Characterization of the peptide-binding motif of a rhesus MHC class I molecule (Mamu-A*01) that binds an immunodominant CTL epitope from SIV. *J. Immunol.* **160,** 6062–6071 (1998).
16. Price, G. E., Ou, R., Jiang, H., Huang, L. & Moskophidis, D. Viral escape by selection of cytotoxic T cell-resistant variants in influenza A virus pneumonia. *J. Exp. Med.* **191,** 1853–1867 (2000).
17. Kimura, M. Preponderance of synonymous changes as evidence for the neutral theory of molecular evolution. *Nature* **267,** 275–276 (1977).
18. Hughes, A. L. & Nei, M. Pattern of nucleotide substitution at major histocompatibility complex class I loci reveals overdominant selection. *Nature* **335,** 167–170 (1988).
19. Allen, T. M. *et al.* Induction of AIDS virus-specific CTL activity in fresh, unstimulated PBL from rhesus macaques vaccinated with a DNA prime/MVA boost regimen. *J. Immunol.* **164,** 4968–4978 (2000).
20. Coffin, J. M. HIV population dynamics *in vivo*: Implications for genetic variation, pathogenesis, and therapy. *Science* **267,** 483–489 (1995).
21. Collins, K. L., Chen, B. K., Kalams, S. A., Walker, B. D. & Baltimore, D. HIV-1 Nef protein protects infected primary cells against killing by cytotoxic T lymphocytes. *Nature* **391,** 397–401 (1998).
22. Cafaro, A. *et al.* Control of SHIV-89.6P-infection of cynomolgus monkeys by HIV-1 Tat protein vaccine. *Nature Med.* **5,** 643–650 (1999).
23. Pauza, C. D. *et al.* Vaccination with Tat toxoid attenuates disease in simian/HIV-challenged macaques. *Proc. Natl Acad. Sci. USA* **97,** 3515–3519 (2000).
24. Osterhaus, A. D. M. E. *et al.* Vaccination with Rev and Tat against AIDS. *Vaccine* **17,** 2713–2714 (1999).
25. Altman, J. D. *et al.* Phenotypic analysis of antigen-specific T lymphocytes. *Science* **274,** 94–96 (1996).
26. Knapp, L. A., Lehmann, E., Piekarczyk, M. S., Urvater, J. A. & Watkins, D. I. A high frequency of *Mamu-A*01* in the rhesus macaque detected by polymerase chain reaction with sequence-specific primers and direct sequencing. *Tissue Antigens* **50,** 657–661 (1997).
27. Regier, D. A. & Desrosiers, R. C. The complete nucleotide sequence of a pathogenic molecular clone of simian immunodeficiency virus. *AIDS Res. Hum. Retroviruses* **6,** 1221–1231 (1990).
28. Nei, M. & Gojobori, T. Simple methods for estimating the numbers of synonymous and nonsynonymous nucleotide substitutions. *Mol. Biol. Evol.* **3,** 418–426 (1986).

Supplementary information is available on *Nature*'s World-Wide Web site (http://www.nature.com) or as paper copy from the London editorial office of *Nature*.

Acknowledgements

We thank L. Smith and B. Becker for preparation of this manuscript and C. D. Pauza and the Immunology and Virology Core Laboratory for infection with molecularly cloned SIV_{MAC239} nef stop and monitoring of macaques. This work was supported by the NIAID, NCRR and the The James B. Pendleton Charitable Trust. D.I.W. is an Elizabeth Glaser scientist.

Correspondence and requests for materials should be addressed to D.I.W. (e-mail: watkins@primate.wisc.edu).

Superoxide dismutase as a target for the selective killing of cancer cells

Peng Huang*, Li Feng*, Elizabeth A. Oldham*, Michael J. Keating† & William Plunkett*

**Department of Experimental Therapeutics, † Department of Leukaemia, The University of Texas M. D. Anderson Cancer Center, 1515 Holcombe Boulevard, Houston, Texas 77030, USA*

Superoxide dismutases (SOD) are essential enzymes that eliminate superoxide radical (O_2^-) and thus protect cells from damage induced by free radicals[1–3]. The active O_2^- production and low SOD activity in cancer cells[3–7] may render the malignant cells highly dependent on SOD for survival and sensitive to inhibition of SOD. Here we report that certain oestrogen derivatives selectively kill human leukaemia cells but not normal lymphocytes. Using complementary DNA microarray and biochemical approaches, we identify SOD as a target of this drug action and show that chemical modifications at the 2-carbon (2-OH, 2-OCH_3) of the derivatives are essential for SOD inhibition and for apoptosis induction. Inhibition of SOD causes accumulation of cellular O_2^- and leads to free-radical-mediated damage to mitochondrial membranes, the release of cytochrome *c* from mitochondria and apoptosis of the cancer cells. Our results indicate that targeting SOD may be a promising approach to the selective killing of cancer cells, and that mechanism-based combinations of